



European Union
European Social Fund



MINISTRY OF EDUCATION & RELIGIOUS AFFAIRS, CULTURE & SPORTS
M A N A G I N G A U T H O R I T Y

Co-financed by Greece and the European Union



EUROPEAN SOCIAL FUND

Program THALIS: INOVBIOMASS: “Development of new material from waste biomass for hydrocarbons adsorption in aquatic environments”

Workpackage WP 5. Factorial experimental design and execution of measurements for determining the parameters affecting the behavior of the novel adsorbent in aquatic solutions and colloidal suspensions of hydrocarbons, salts and dyes

Activity 5.1 Factorial experimental design and execution of measurements for determining the parameters affecting the thermochemical treatment of biomass and the adsorption/desorption of hydrocarbons, also including kinetic models for material degradation due to ageing/deterioration (to account for degradation at storage/transfer)

Interim Technical Report

Title: Execution of measurements for determining the parameters affecting the thermochemical treatment of biomass and the adsorption/desorption of dyes - Part II: Brine treated biomass

By Odysseas N. Kopsidas

Piraeus, December 2013

This research has been co-financed by the European Union (European Social Fund - ESF) and Greek national funds through the Operational Program "Education and Lifelong Learning" of the National Strategic Reference Framework (NSRF) - Research Funding Program: THALIS - UNIVERSITY OF PIRAEUS - DEVELOPMENT OF NEW MATERIAL FROM WASTE BIOMASS FOR HYDROCARBONS ADSORPTION IN AQUATIC ENVIRONMENTS.



European Union
European Social Fund



MINISTRY OF EDUCATION & RELIGIOUS AFFAIRS, CULTURE & SPORTS
M A N A G I N G A U T H O R I T Y

Co-financed by Greece and the European Union



EUROPEAN SOCIAL FUND

Table of Contents

Table of Contents	2
Introduction	3
2. Materials and Methods	5
2.1. Materials	5
2.2 Pretreatments.....	5
2.3. Continuous fixed-bed column studies	6
2.3.1. Adsorption studies	6
3. Results and Discussion.....	6
3.1. Continuous fixed-bed-column adsorption model.....	6
3.2. Continuous fixed-bed-column desorption model.....	9
3.3. Brine treated.....	9
3.4. Continuous fixed-bed-column models parameters.....	11
4. References	29



European Union
European Social Fund



MINISTRY OF EDUCATION & RELIGIOUS AFFAIRS, CULTURE & SPORTS
M A N A G I N G A U T H O R I T Y



Co-financed by Greece and the European Union

Introduction

Brine is a solution of salt (usually sodium chloride) in water. In different contexts, brine may refer to salt solutions ranging from about 3.5% (a typical concentration of seawater, or the lower end of solutions used for brining foods) up to about 26% (a typical saturated solution, depending on temperature). Brine is a liquid. 0 °F was initially set as the zero point in the Fahrenheit temperature scale, as it was the coldest temperature that Daniel Gabriel Fahrenheit could reliably reproduce — by freezing brine. At 100 °C (373.65 K, 212 °F), saturated sodium chloride brine is about 28% salt by weight i.e. 39.12 g salt dissolves in 100 mL of water at 100 °C. At 0 °C (273.15 K, 32 °F), brine can only hold about 26% salt. Brine is a common fluid used in large refrigeration installations for the transport of thermal energy from place to place. It is used because the addition of salt to water lowers the freezing temperature of the solution and the heat transport efficiency can be greatly enhanced for the comparatively low cost of the material. The lowest freezing point obtainable for NaCl brine is $-21.1\text{ }^{\circ}\text{C}$ ($-6.0\text{ }^{\circ}\text{F}$) at 23.3wt% NaCl. This is called the eutectic point. [1,2].

According to many review papers [3], [4], [5], [6], [7] and [8] low-cost adsorbents offer a lot of promising benefits for commercial purposes in the future. They could be used in place of commercial activated carbon for the removal of dyes in aqueous solutions.

Many industries, such as paper, plastics, food, printing, leather, cosmetics and textile, use dyes in order to color their products [1]. In textile industries about 10–15% of the dye gets lost in the effluent during the dyeing process which are harmful products and may cause cancer epidemics [2- 3]. Dyes usually have a synthetic origin and complex aromatic molecular structures which make them more stable and more difficult to biodegrade [1- 4]. The industrial runoffs are usually discarded into rivers and lakes, altering the biological stability of surrounding ecosystems [5]. Therefore, removal of dyestuffs from wastewater has received considerable attention over the past decades.



Co-financed by Greece and the European Union

In wastewater treatment, various methods applied to remove dyes include photocatalytic degradation [6], membrane separation [7], chemical oxidations [8] and electrochemical process. Among the above mentioned techniques of dye removal, the process of adsorption gives the best results as it can be used to remove different types of coloring materials [10].

Adsorption onto activated carbon is the most widespread technology for the removal of pollutants from water and wastewaters. The disadvantage of activated carbon is its high cost [11]. Hence, it is of pivotal importance thence of low-cost substitute adsorbents to replace activated carbons. Various types of untreated biomass have been reported to have a use in dye removal: sawdust [9] and [11], wheat straw [12], cedar sawdust [13], rubberwood sawdust [14], kudzu [15], banana and orange peels [16] and palm kernel fiber [17, 11], peanut husk [4], palm kernel fibre [11], *Turbinaria turbinata* alga [12], graphene [13], defatted jojoba [14] and sugar bet pulp [15].

Further, numerous pretreated lignocellulosic materials are used to remove dyes in water and wastewater. Pyrolyzed date pits [16], date stones [17] and *Turbinaria turbinata* alga [12] have proved to be effective adsorbents. Acid and alkali pretreated lignocellulosic materials (wheat straw, corncobs, barley husks, wood sawdust) were successfully used as adsorbents for a variety of dyes [18], [19] and [20]. Prehydrolysed (with dilute sulphuric acid aquatic solution at 100 °C) wheat straw [12] and beech sawdust [21] and chloride salts treated (at 100 °C) beech sawdust [9] and [11] has been proven to be effective for basic dyes adsorption in batch and fixed-bed systems.

In this study continuous fixed-bed-column systems were investigated. The adsorbents which we use are: spruce (*Picea Abies*) untreated and spruce modified by brine treatment. The column systems were filed with biomass at various initial dye concentrations, flow rates and bed-depths. The column kinetics of Methylene Blue (MB) adsorption on spruce (*Picea Abies*) untreated, and spruce modified by brine treatment, was simulated herein, using biomass as control, in order to facilitate its potential use as a low cost adsorbent for wastewater dye removal. Economies arise

when the facility that can use such adsorption materials is near a source of a lignocellulosic waste as agricultural residues, thus saving transportation cost and contributing to industrial ecology at local level.

2. Materials and Methods

2.1. Materials

In this study continuous fixed-bed-column systems were investigated. The adsorbents which we use are: spruce (*Picea Abies*) untreated, spruce modified by autohydrolysis. The column systems were filed with biomass at various initial dye concentrations, flow rates and bed-depths. The column kinetics of Methylene Blue (MB) adsorption on spruce (*Picea Abies*) untreated, spruce modified by autohydrolysis. Economies arise when the facility that can use such adsorption materials is near a source of a lignocellulosic waste as agricultural residues, thus saving transportation cost and contributing to Industrial Ecology at local level.

2.2 Pretreatments

The brine treatment process was performed in a 3.75-L batch reactor PARR 4843. The isothermal autohydrolysis time was $t_{ai} = 0, 10, 20, 30, 40$ and 50 min (not including the non-isothermal preheating and the cooling time-periods); the reaction was catalyzed by the organic acids produced by the pine sawdust itself during autohydrolysis at a liquid-to-solid ratio of 10:1; the liquid phase volume (water) was 2000 mL and the solid material dose (pine sawdust) was 200 g; stirring speed 150 rpm. The reaction ending temperature values were $T = 160$ °C, 200 °C and 240 °C, reached after $t = 42, 62$ and 80 min preheating time values, respectively. The autohydrolysis product was filtered using a Buchner filter with Munktell paper sheet (grade 34/N) to separate the liquid phase and from the solid phase. The solid residue was washed with water until neutral pH (the

initial filtrate pH was 2.90–4.76 depending on the autohydrolysis severity). The solid residue was dried at 110 °C for 10 days at room temperature to reach the humidity of the untreated material. Then it was used as adsorbent.

2.3. Continuous fixed-bed column studies

2.3.1. Adsorption studies

Continue-flow experiments were carried out on Stainless steel columns with dimensions 15 X 2.5 cm. The bed height was $x = 15$ cm respectively. The adsorbent weight was $m = 32$ g and 54 g, respectively. The pH was 8.0. The flow rates were fixed at approximately 20 mL min⁻¹ using a preparative HPLC pump, LaPrep P110 - VWR - VWR International. The initial concentrations of MB were 165 mg L⁻¹. To determine the concentration of MB in the effluent, samples of outflow were peaked at 100 mL intervals.

3. Results and Discussion

3.1. Continuous fixed-bed-column adsorption model

A widely used continuous fixed-bed-column model was established by Bohart and Adams [28], who assumed that the rate of adsorption is controlled by the surface binding (through chemical reaction or physical interaction) between adsorbate and unused capacity of the solid, i.e., adsorption rate = $K C C_u$, where K is the adsorption rate coefficient, C is the adsorbate concentration at the solid phase at distance x , and C_u is the unused surface adsorptive capacity at time t , expressed as mass per volume of bed. The material balance for adsorbate is given by the partial differential equation

$$\frac{\partial C_u}{\partial t} = -K \cdot C \cdot C_u \quad (1)$$

while the corresponding partial differential equation for the C_u decrease is

$$\frac{\partial C}{\partial x} = -\frac{K}{u} \cdot C \cdot C_u \quad (2)$$

where u is the superficial liquid velocity. These equations are obtained neglecting diffusion and accumulation terms, assumptions that are valid in chemical engineering practice, provided that strict scale up specifications are kept in the design stage and successful operation conditions are kept in the industrial operation stage.

The differential equations can be integrated over the total length x of the bed to give:

$$\ln\left(\frac{C_i}{C} - 1\right) = \ln\left[\exp\left(\frac{K \cdot N \cdot x}{u}\right) - 1\right] - K \cdot C_i \cdot t \quad (3)$$

where N (mg L^{-1}); is the initial or total adsorption capacity coefficient, also quoted as $C_{u,0}$ [28]; C =effluent concentration (mg L^{-1}); C_i =influent concentration (mg L^{-1}); K =adsorption rate coefficient ($L \cdot \text{mg}^{-1} \cdot \text{min}^{-1}$); x =bed depth (cm); u =linear velocity (cm min^{-1}); and t =time (min). Since $\exp(K \cdot N \cdot x / u)$ is usually much greater than unity, this equation can be simplified to:

$$\ln\left(\frac{C_i}{C} - 1\right) = \frac{K \cdot N \cdot x}{u} - K \cdot C_i \cdot t \quad (4)$$

which is commonly used by researchers, because of its convenience in estimating the values of parameters K and N through linear regression either of $\ln[(C_0 / C_i) - 1]$ vs t or t vs x when the following rearrangement is adopted:

$$t = \frac{N \cdot x}{C_i \cdot u} - \frac{1}{K \cdot C_i} \cdot \left(\ln \frac{C_i}{C} - 1 \right) \quad (5)$$

In this rearrangement, t is the time to breakthrough, i.e., the time period required for concentration to reach a predetermined value. For using the last expression as a linear regression model, wastewater is passed through beds of varying depths, keeping constant C_i and u , preferably at values similar to those expected to prevail under real conditions at full scale. Alternatively, it can be performed by the aid of at least three columns arranged in series. In such a case, sampling takes place at the bottom of each column and measured for adsorbate concentration, making more frequent measurements when approaching the breakthrough concentration C . Finally, the time at which the effluent reaches this concentration is used as the dependent variable while x plays the role of the independent one. Evidently, the use of such a regression model implies the additional error of measuring the independent variable with less precision in comparison with the dependent. The common error in both models comes from the estimation of concentration from measuring adsorbance although the reference relation/curve has been structured/drawn in the inverse mode, i.e., for predetermined concentrations the corresponding adsorbances have been measured.

In the present work, the model of eq. (17) has been used for parameter values estimation through linear regression to obtain numerical results comparable with corresponding data found for other fixed bed adsorption studies in literature. The non-linear form of this model is:

$$C = \frac{C_i}{1 + Ae^{-rt}} \quad (6)$$

where $A = e^{K \cdot N \cdot x / u}$; $r = K \cdot C_i$.

On the other hand, Clark [29] has advanced the Bohart and Adams model [28] by incorporating the parameter n of the Freundlich adsorption isotherm:

$$C = \left[\frac{C_i^{n-1}}{1 + Ae^{-rt}} \right]^{\frac{1}{n-1}} \quad (7)$$

where n =inverse of the slope of the Freundlich isotherm [22]. Finally, the Bohart and Adams model [28] can be reduced for $n=2$ from Clark model [29].

3.2. Continuous fixed-bed-column desorption model

The kinetic equation used for desorption is the following:

$$C = C'_0 e^{-k't'} \quad (21)$$

where C'_0 is the initial MB concentration of desorption effluent, k' is desorption rate constant assuming first order desorption kinetics and t' is desorption time.

3.3. Brine treated

The use of salt brine — a mixture of 23 percent salt and 77 percent water (the carrying capacity of salt in a water solution) — for melting snow and ice was developed in Europe. The mixture is sprayed directly on the road as an anti-icing agent. Although salt brine has the same melting characteristics of regular salt, because it is in brine form, it has the advantage of working immediately and doesn't have the problem of “bounce and scatter” off the road because of its consistency, according to a study of salt brine use by the Vermont Agency of Transportation, Materials and Research Section. The agency found that brine was cost effective to produce, at about \$0.10 per gallon. Additionally, other deicing chemicals can be mixed into the salt brine to lower the

effective melting temperature. During the study in which experimental test sections of Vermont interstates were treated with salt brine and salt brine mixtures, the agency found that it saved an average of 24 percent of material usage.

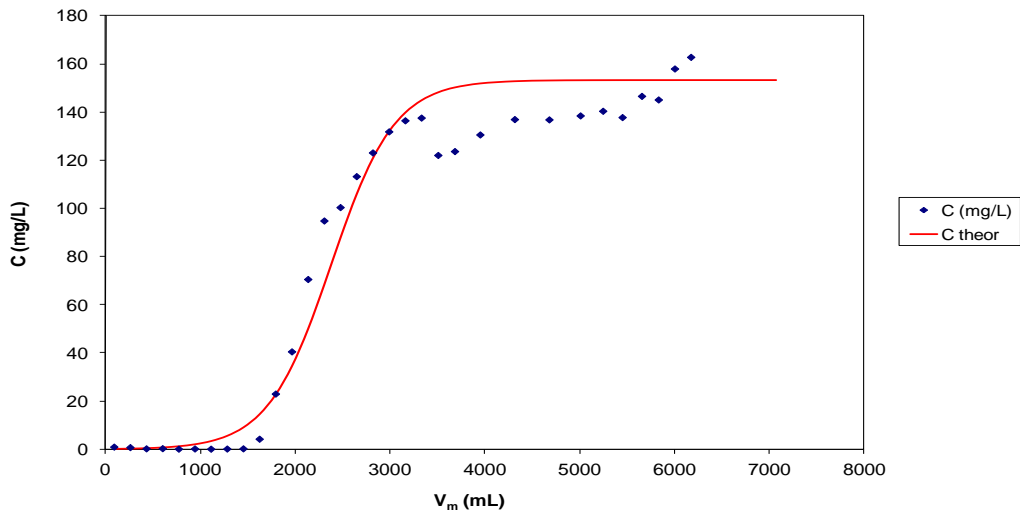
Although the data sets were not as extensive as the research team initially thought, the research project was able to produce salt savings of approximately 30 percent and materials cost savings of approximately 30 percent and materials cost savings of approximately 24 percent during the first year of experimentation,” according to the Vermont DOT report. If such a cost savings could be projected statewide, the potential savings would be almost \$1 million annually. The research team agreed that there is potential for more salt and cost savings as staff becomes more experienced with the technology.



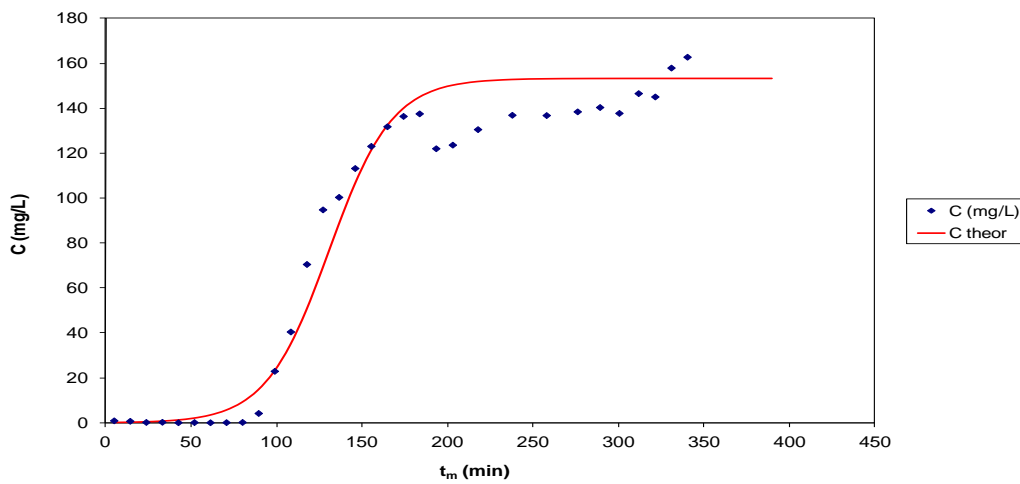
3.4. Continuous fixed-bed-column models parameters

Table 1: Fixed Bed Column Systems for spruce modified by brine treatment

Concen trated X Times	T (oC)	t (min)	Ci	Q (mL/min)	x (cm)	m (g)	N	K	R	qo (mg/g)
1	180	50	153	18	15	20	4948	0.000353	-0.9481	18.21
2	180	50	145	21	15	20	6975	0.000242	-0.9683	25.67
4	140	0	210	21	15	12.11	8461	0.000153	-0.9616	51.42
4	160	0	156	21	15	11.7	4304	0.000694	-0.9946	27.07
4	160	50	163	21	15	20	5834	0.000300	-0.9662	21.47
4	180	0	162	21	15	11.6	6054	0.000257	-0.9744	38.41
4	180	50	151	21	15	20	5666	0.000444	-0.9479	20.85
4	200	0	155	22	15	12.3	4682	0.000866	-0.9667	28.01
4	200	50	162	21	15	14.6	9259	0.000132	-0.9390	46.67
4	200	50	148	21	15	20	7713	0.000157	-0.9232	28.38
4	220	50	157	21	15	12	5840	0.000235	-0.9863	35.82
4	200	50	160	21	15	20	9233	0.000181	-0.9466	33.97
4	240	50	162	19	15	13	1358	0.000899	-0.9237	7.69
4	240	50	153	21	15	12	451	0.000369	-0.7918	2.76
4	240	50	153	21	15	12	451	0.000369	-0.7918	2.76
8	180	0	169	21	15	12	4715	0.000212	-0.9565	28.92
8	180	50	159	17	15	17.3	7089	0.000351	-0.9211	30.16
8	180	50	141	21	15	20	5695	0.000259	-0.9799	20.96

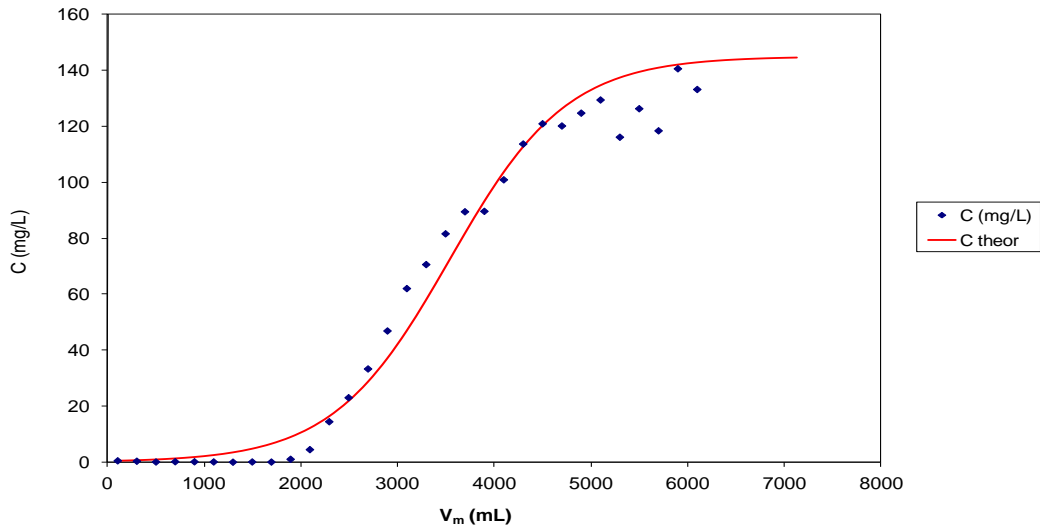


(a)

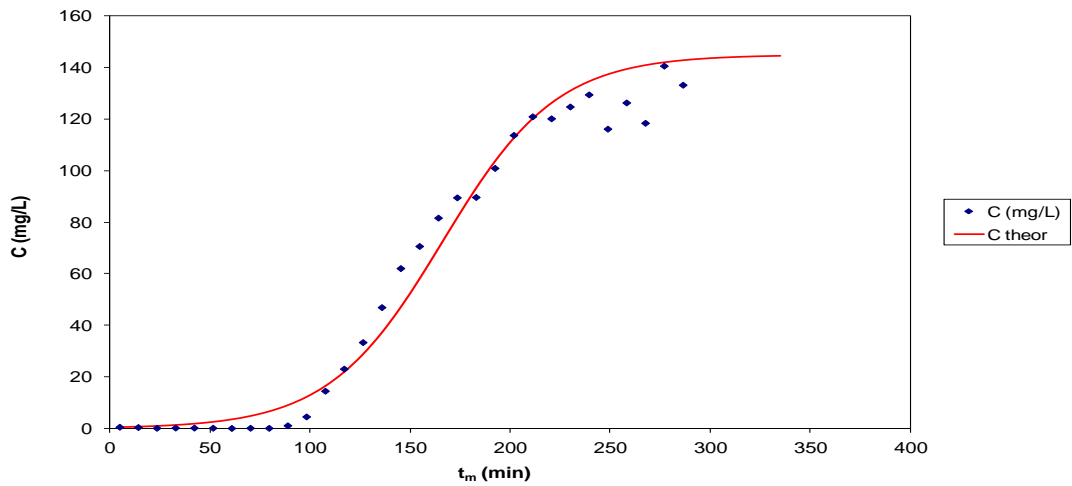


(b)

Fig. 1: Column experimental data and theoretical curves of MB adsorption on modified spruce; the effluent concentration is presented vs. (a) the effluent volume and (b) the adsorption time; $x=15\text{cm}$, $C_i=160\text{ mg L}^{-1}$, $Q=20\text{ mL min}^{-1}$, (the theoretical curves are according to the Bohart and Adams model); modified by brine treatment; concentrated x 1 time at $180\text{ }^\circ\text{C}$ for 50 min.



(a)



(b)

Fig. 2: Column experimental data and theoretical curves of MB adsorption on modified spruce; the effluent concentration is presented vs. (a) the effluent volume and (b) the adsorption time; $x=15\text{cm}$, $C_i=160\text{ mg L}^{-1}$, $Q=20\text{ mL min}^{-1}$, (the theoretical curves are according to the Bohart and Adams model); modified by brine treatment; concentrated x 2 times at $180\text{ }^\circ\text{C}$ for 50 min.

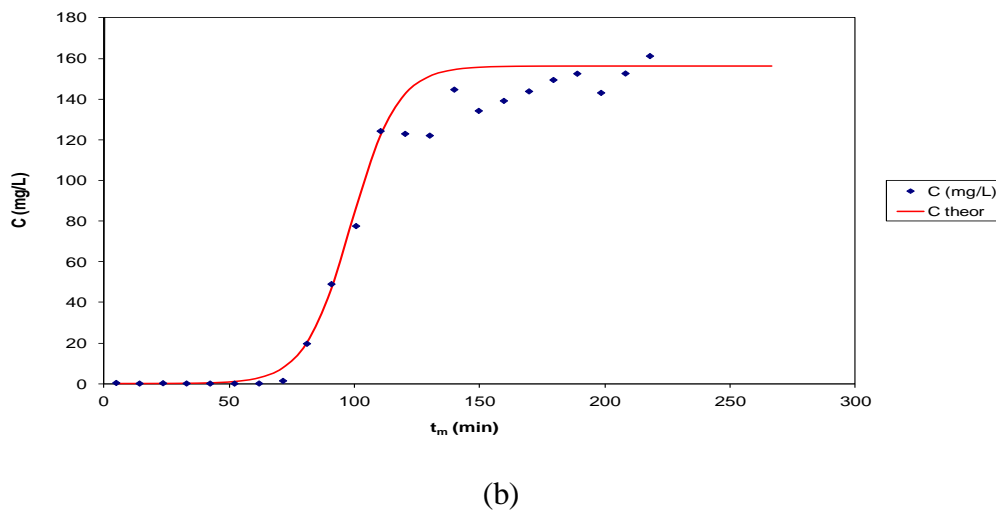
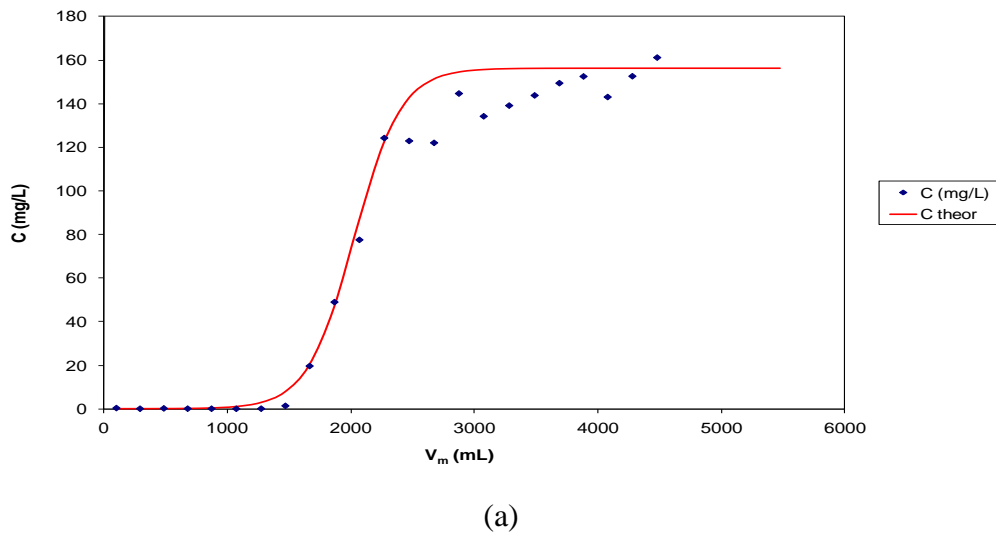
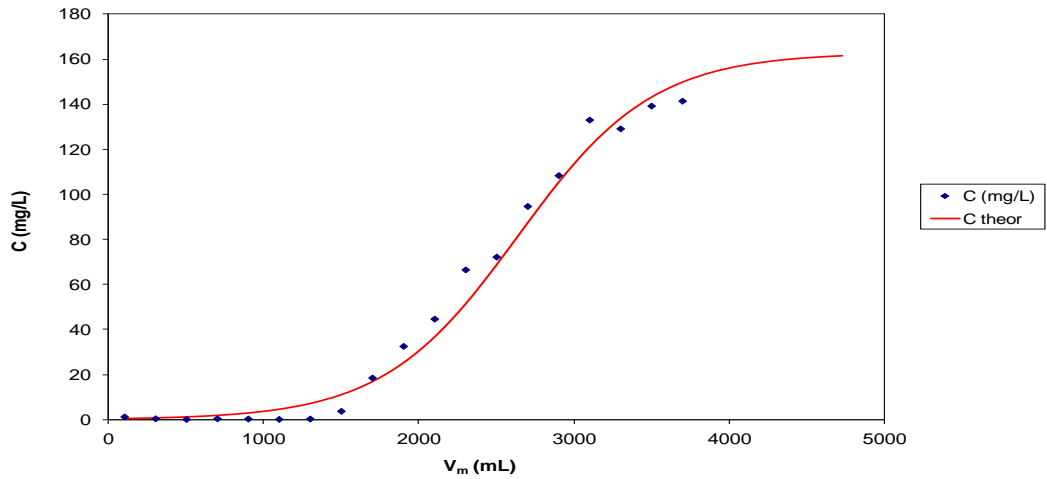
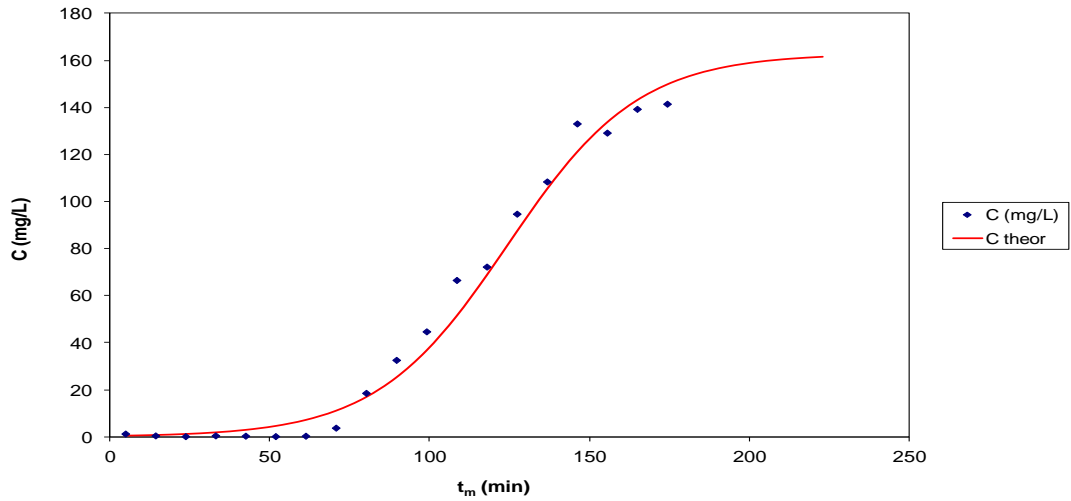


Fig. 3: Column experimental data and theoretical curves of MB adsorption on modified spruce; the effluent concentration is presented vs. (a) the effluent volume and (b) the adsorption time; $x=15\text{cm}$, $C_i=160\text{ mg L}^{-1}$, $Q=20\text{ mL min}^{-1}$, (the theoretical curves are according to the Bohart and Adams model); modified by brine treatment; concentrated x 2 times at $160\text{ }^\circ\text{C}$ for 0 min.

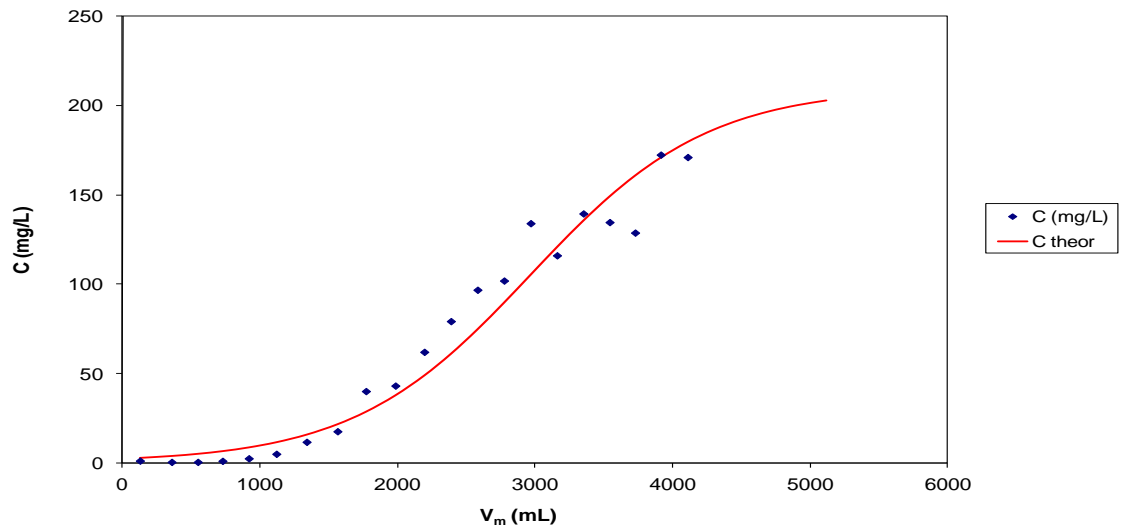


(a)

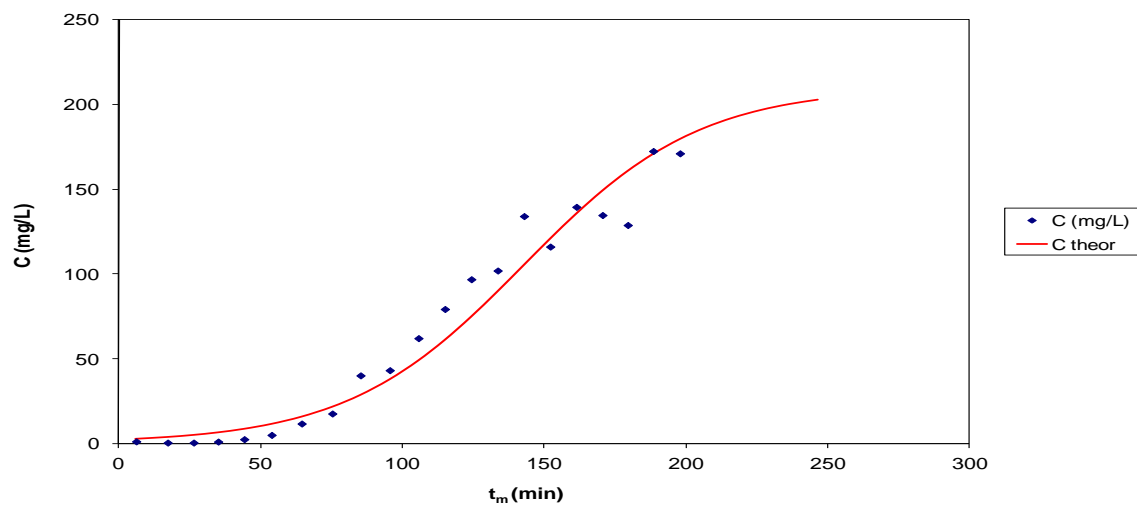


(b)

Fig. 4: Column experimental data and theoretical curves of MB adsorption on modified spruce; the effluent concentration is presented vs. (a) the effluent volume and (b) the adsorption time; $x=15\text{cm}$, $C_i=160\text{ mg L}^{-1}$, $Q=20\text{ mL min}^{-1}$, (the theoretical curves are according to the Bohart and Adams model); modified by brine treatment; concentrated x 2 times at $160\text{ }^\circ\text{C}$ for 50 min.



(a)



(b)

Fig. 5: Column experimental data and theoretical curves of MB adsorption on modified spruce; the effluent concentration is presented vs. (a) the effluent volume and (b) the adsorption time; $x=15\text{cm}$, $C_i=160\text{ mg L}^{-1}$, $Q=20\text{ mL min}^{-1}$, (the theoretical curves are according to the Bohart and Adams model); modified by brine treatment; concentrated x 4 times at $140\text{ }^\circ\text{C}$ for 0 min.

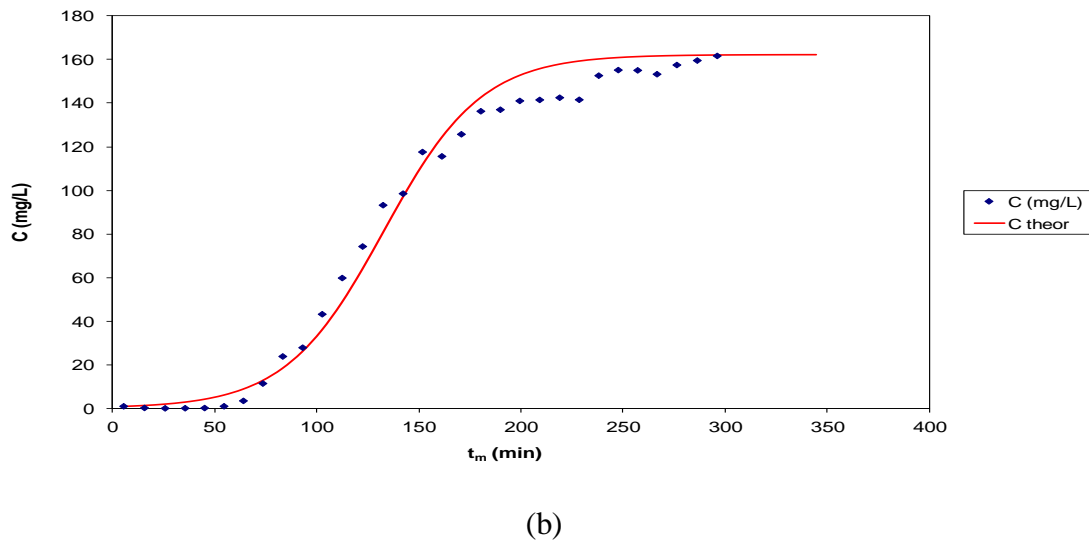
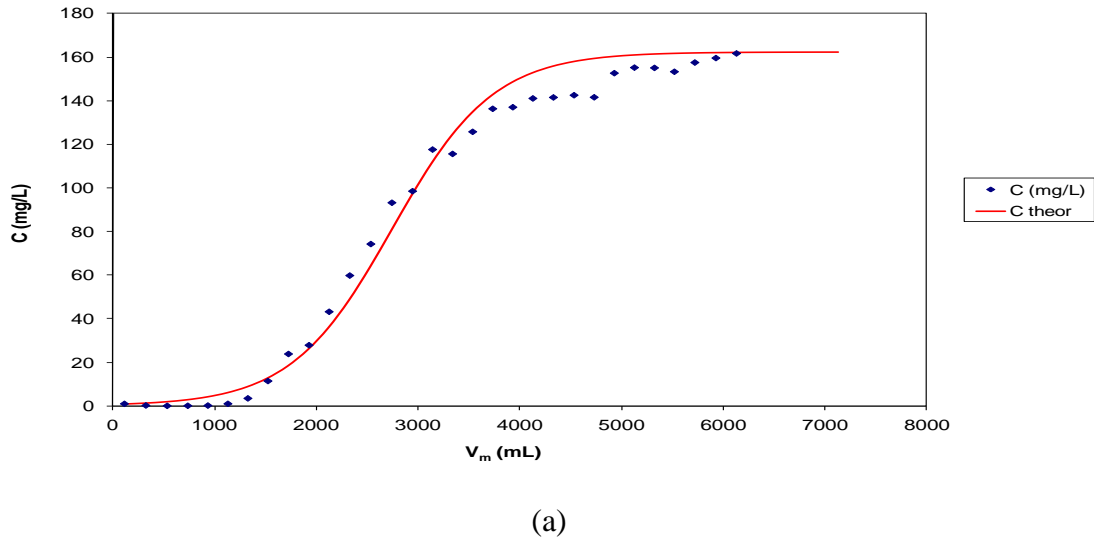
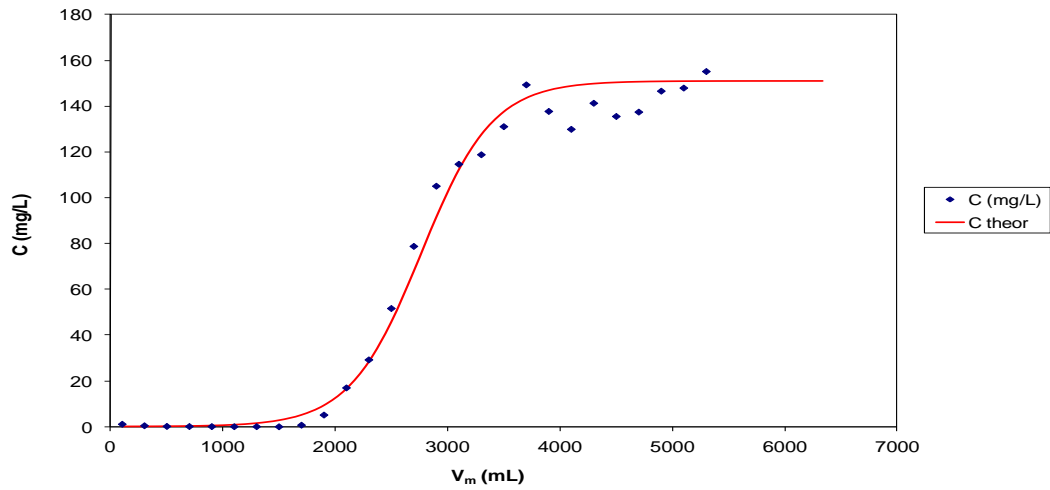
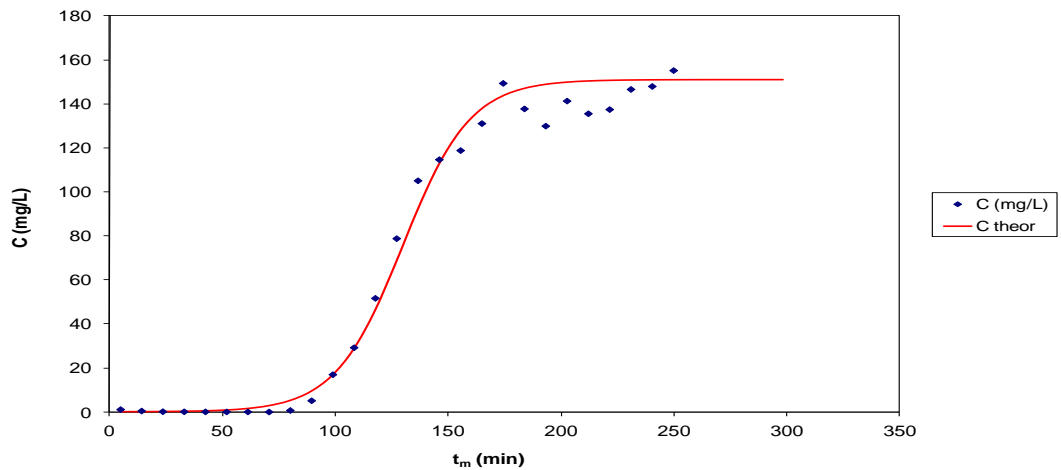


Fig. 6: Column experimental data and theoretical curves of MB adsorption on modified spruce; the effluent concentration is presented vs. (a) the effluent volume and (b) the adsorption time; $x=15\text{cm}$, $C_i=160\text{ mg L}^{-1}$, $Q=20\text{ mL min}^{-1}$, (the theoretical curves are according to the Bohart and Adams model); modified by brine treatment; concentrated x 4 times at $180\text{ }^\circ\text{C}$ for 0 min.

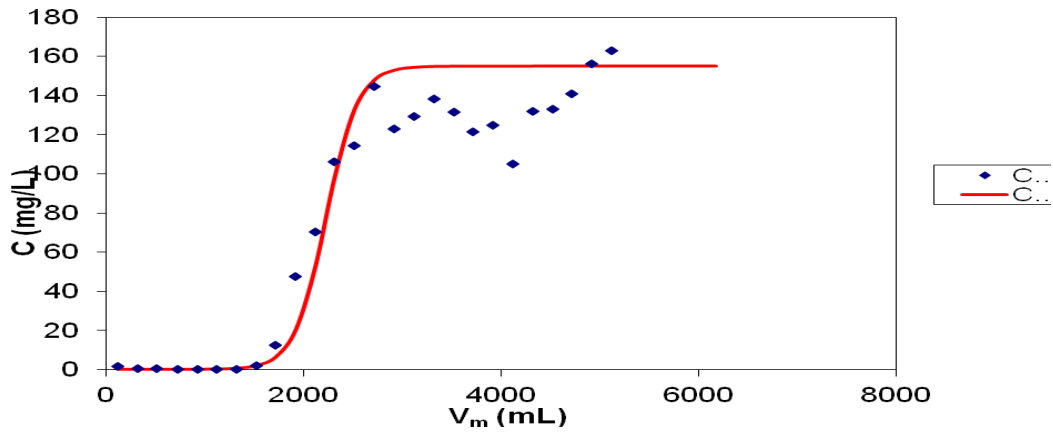


(a)

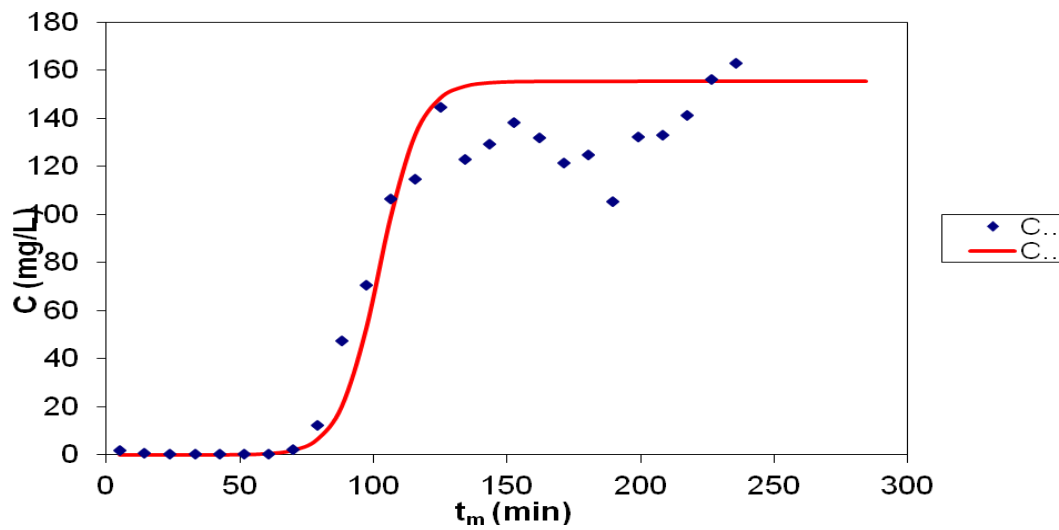


(b)

Fig. 7: Column experimental data and theoretical curves of MB adsorption on modified spruce; the effluent concentration is presented vs. (a) the effluent volume and (b) the adsorption time; $x=15\text{cm}$, $C_i=160\text{ mg L}^{-1}$, $Q=20\text{ mL min}^{-1}$, (the theoretical curves are according to the Bohart and Adams model); modified by brine treatment; concentrated x 4 times at $180\text{ }^\circ\text{C}$ for 50 min.

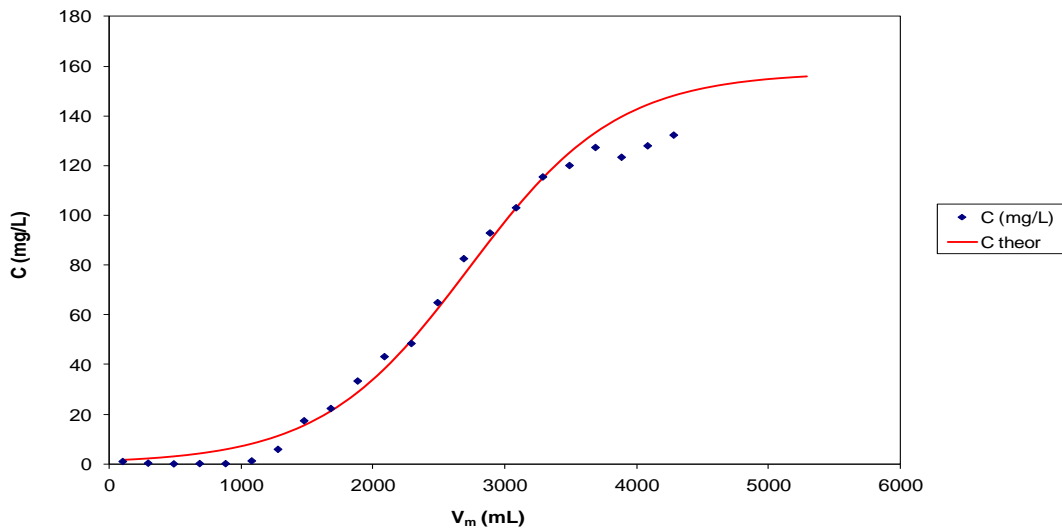


(a)

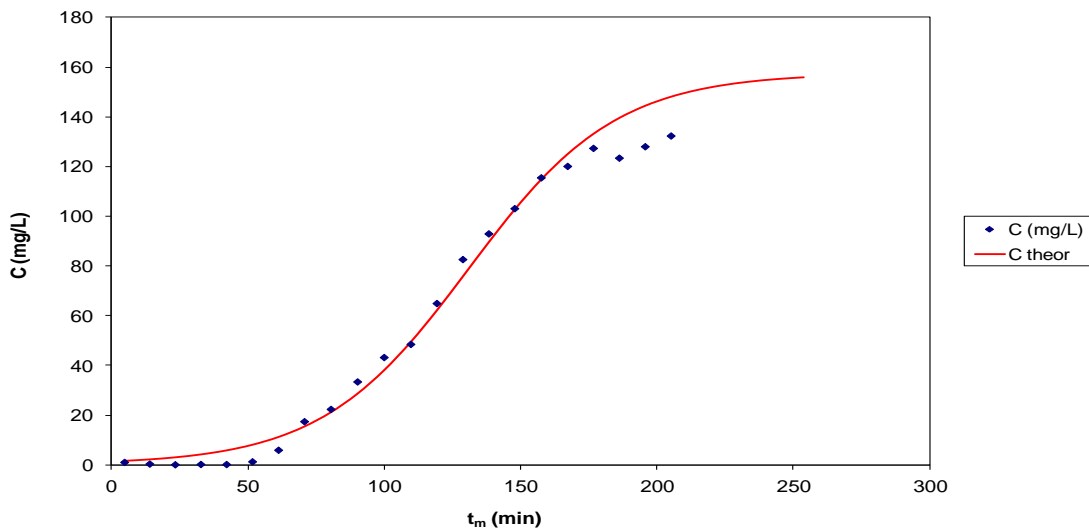


(b)

Fig. 8: Column experimental data and theoretical curves of MB adsorption on modified spruce; the effluent concentration is presented vs. (a) the effluent volume and (b) the adsorption time; $x=15\text{cm}$, $C_i=160\text{ mg L}^{-1}$, $Q=20\text{ mL min}^{-1}$, (the theoretical curves are according to the Bohart and Adams model); modified by brine treatment; concentrated x 4 times at $200\text{ }^\circ\text{C}$ for 0 min.

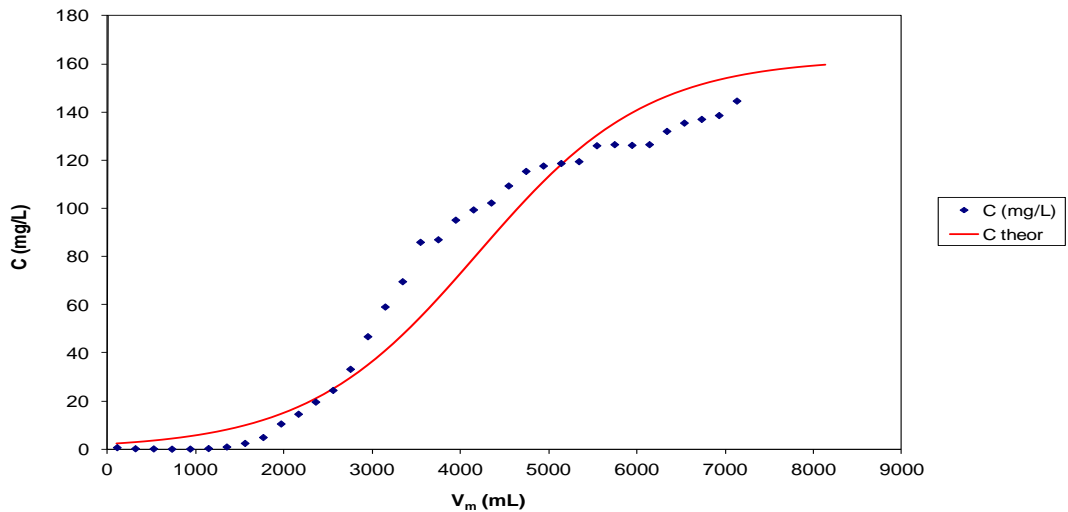


(a)

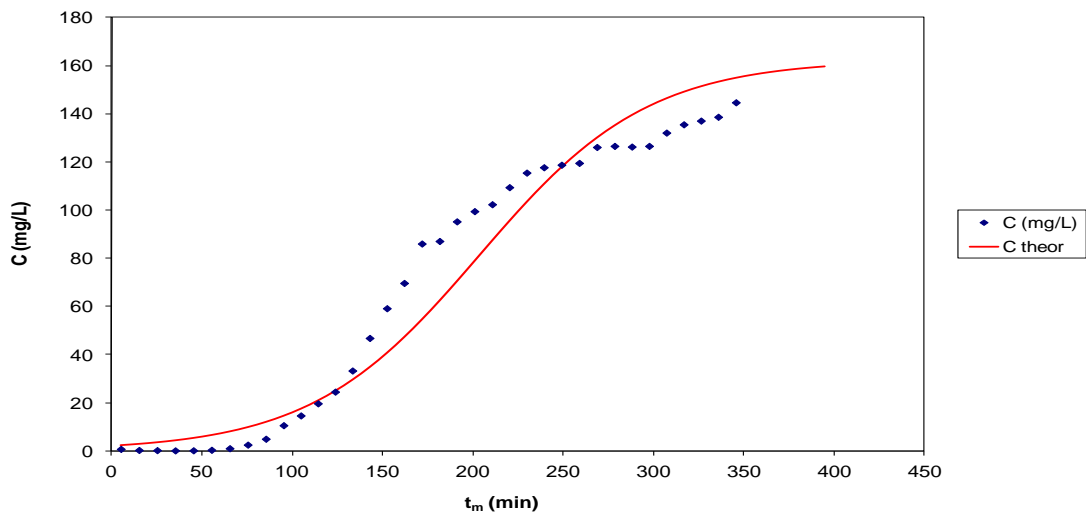


(b)

Fig. 9: Column experimental data and theoretical curves of MB adsorption on modified spruce; the effluent concentration is presented vs. (a) the effluent volume and (b) the adsorption time; $x=15\text{cm}$, $C_i=160\text{ mg L}^{-1}$, $Q=20\text{ mL min}^{-1}$, (the theoretical curves are according to the Bohart and Adams model); modified by brine treatment; concentrated x 4 times at $200\text{ }^\circ\text{C}$ for 50 min.

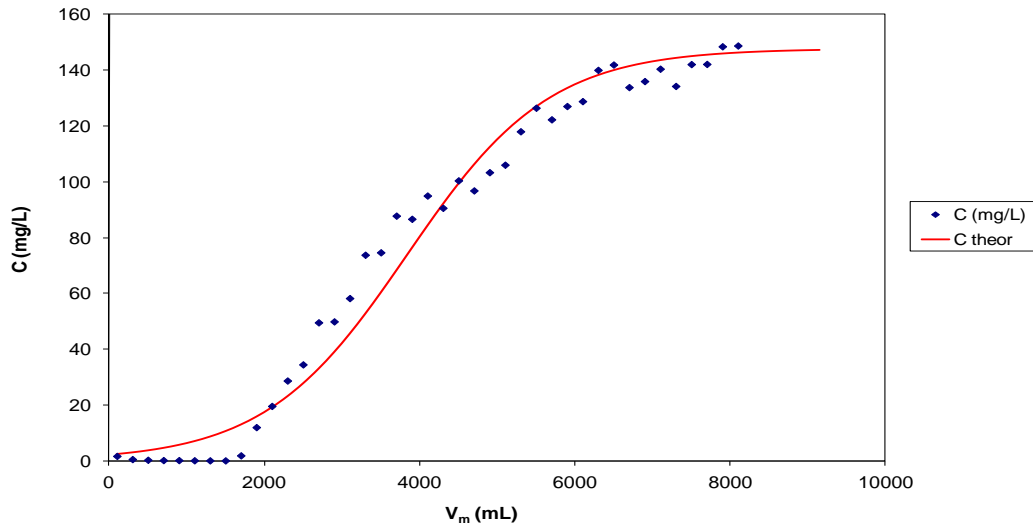


(a)

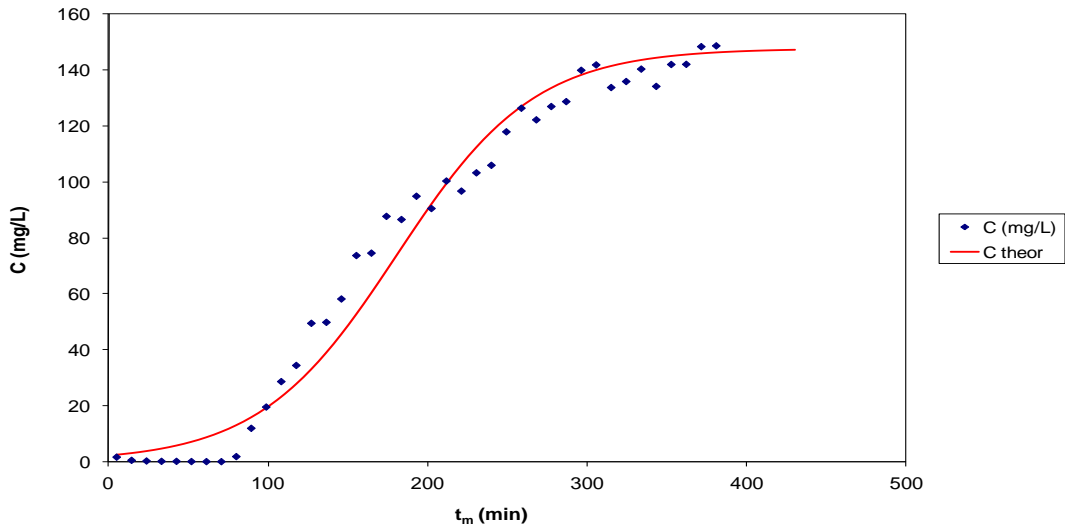


(b)

Fig. 10: Column experimental data and theoretical curves of MB adsorption on modified spruce; the effluent concentration is presented vs. (a) the effluent volume and (b) the adsorption time; $x=15\text{cm}$, $C_i=160\text{ mg L}^{-1}$, $Q=20\text{ mL min}^{-1}$, (the theoretical curves are according to the Bohart and Adams model); modified by brine treatment; concentrated x 4 times at $220\text{ }^\circ\text{C}$ for 50 min.

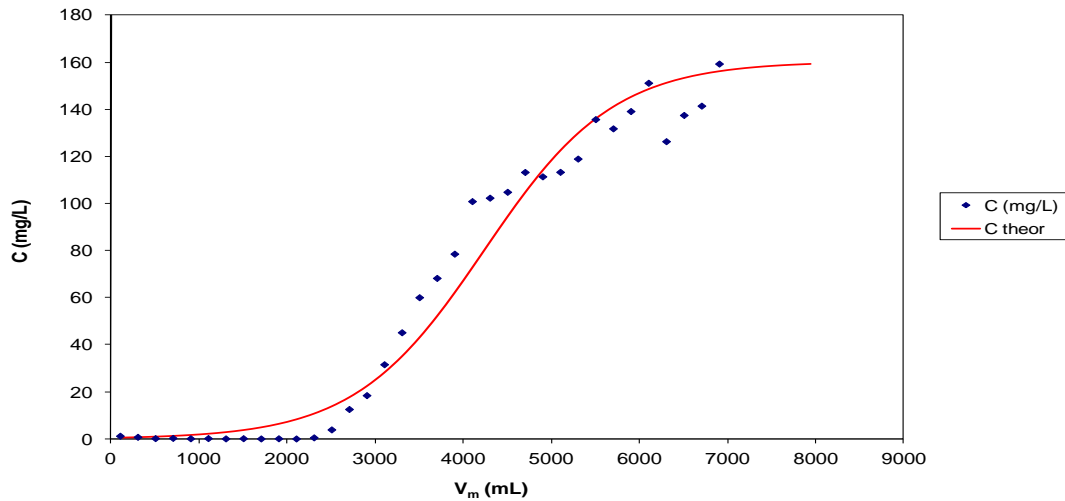


(a)

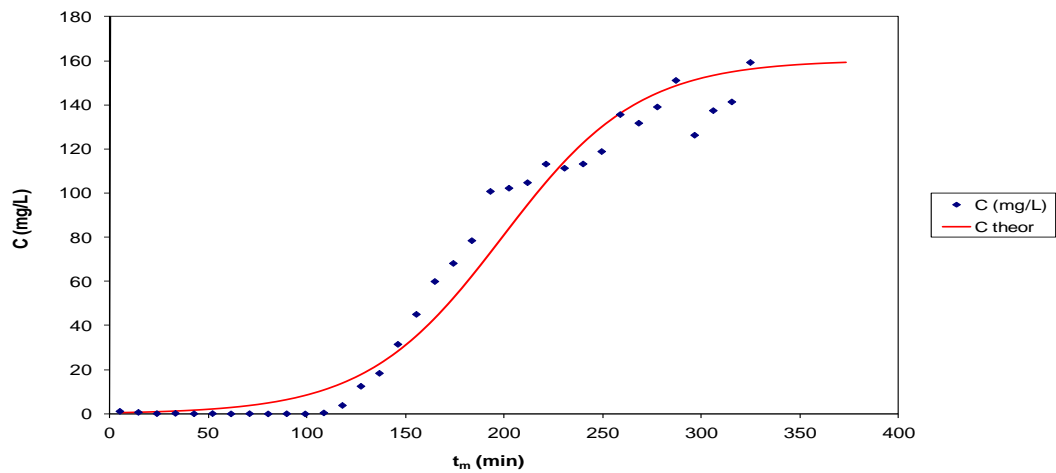


(b)

Fig. 11: Column experimental data and theoretical curves of MB adsorption on modified spruce; the effluent concentration is presented vs. (a) the effluent volume and (b) the adsorption time; $x=15\text{cm}$, $C_i=160\text{ mg L}^{-1}$, $Q=20\text{ mL min}^{-1}$, (the theoretical curves are according to the Bohart and Adams model); modified by brine treatment; concentrated x 4 times at $240\text{ }^\circ\text{C}$ for 50 min.

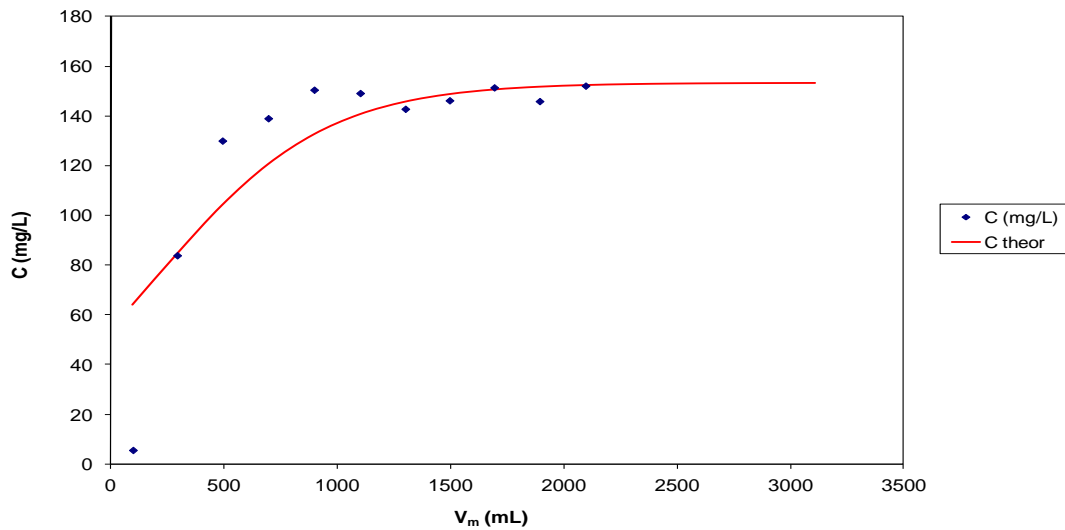


(a)

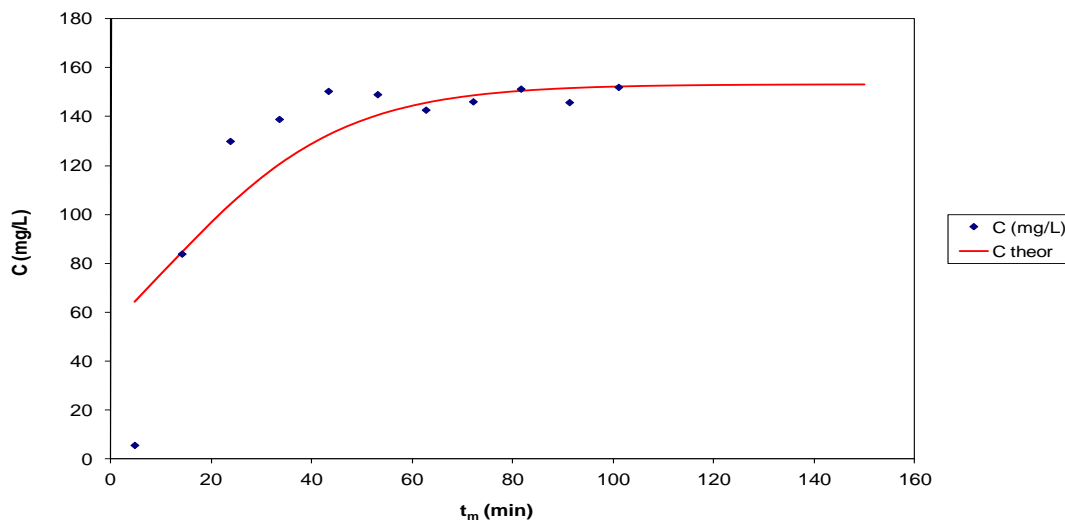


(b)

Fig. 12: Column experimental data and theoretical curves of MB adsorption on modified spruce; the effluent concentration is presented vs. (a) the effluent volume and (b) the adsorption time; $x=15\text{cm}$, $C_i=160\text{ mg L}^{-1}$, $Q=20\text{ mL min}^{-1}$, (the theoretical curves are according to the Bohart and Adams model); modified by brine treatment; concentrated x 4 times at $240\text{ }^\circ\text{C}$ for 50 min (repeatability).

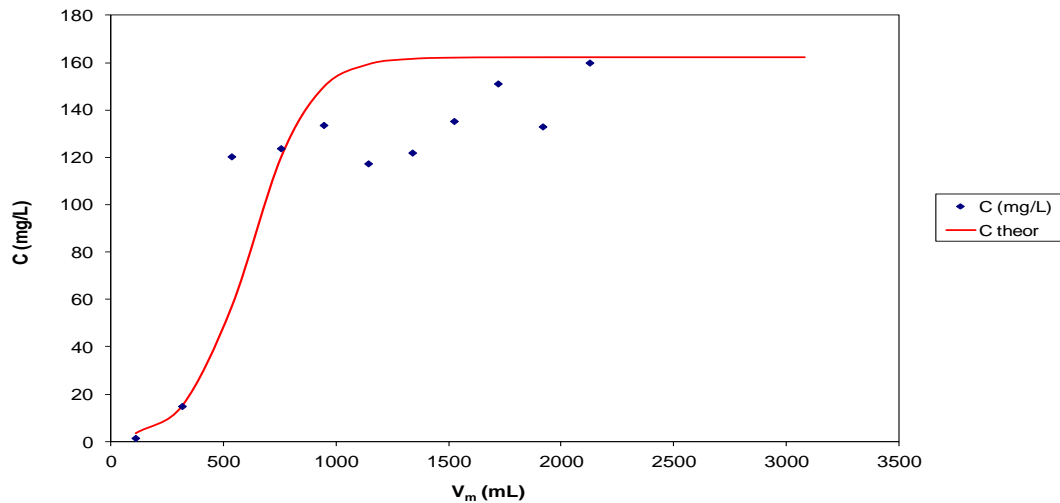


(a)

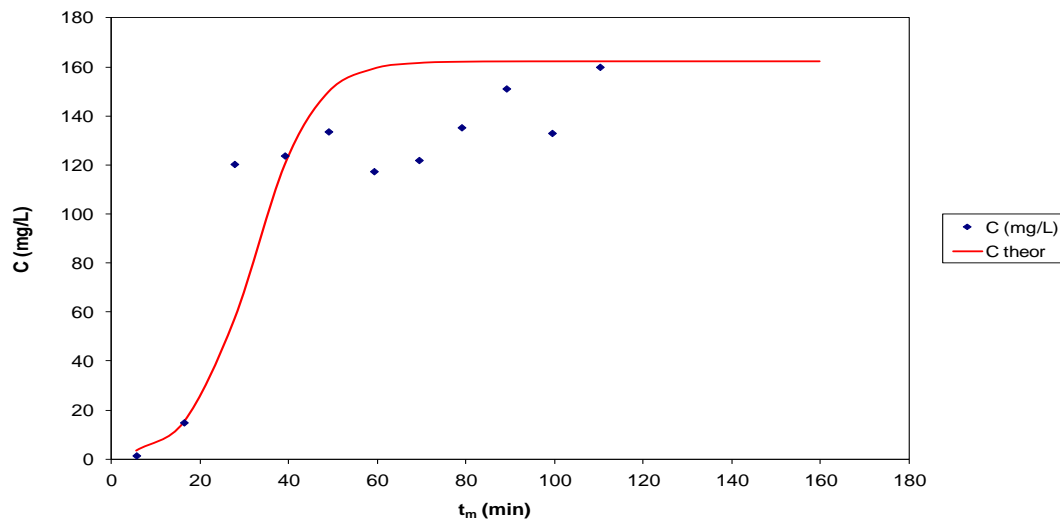


(b)

Fig. 13: Column experimental data and theoretical curves of MB adsorption on modified spruce; the effluent concentration is presented vs. (a) the effluent volume and (b) the adsorption time; $x=15\text{cm}$, $C_i=160\text{ mg L}^{-1}$, $Q=20\text{ mL min}^{-1}$, (the theoretical curves are according to the Bohart and Adams model); modified by brine treatment; concentrated x 4 times at $240\text{ }^\circ\text{C}$ for 50 min.

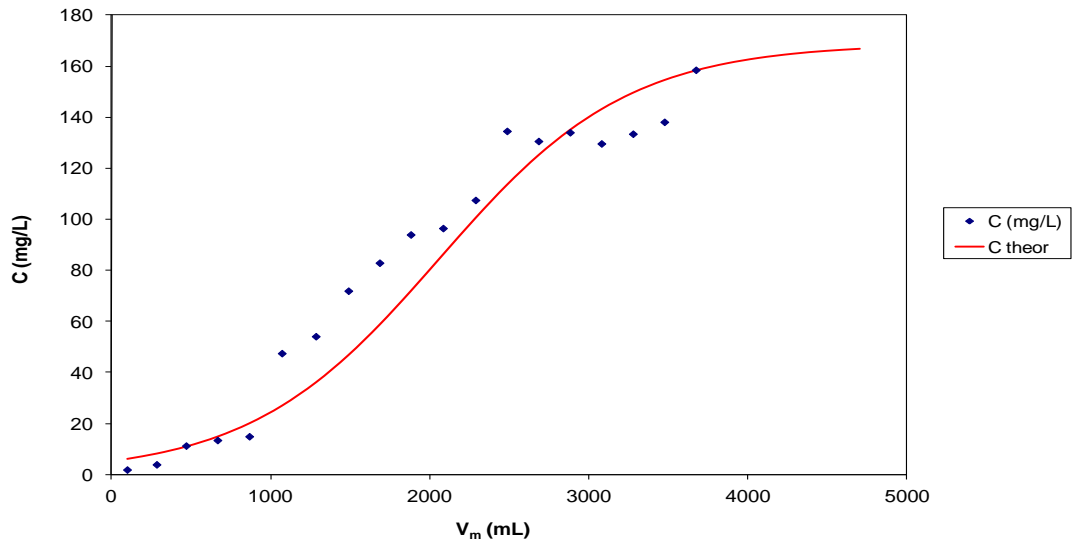


(a)

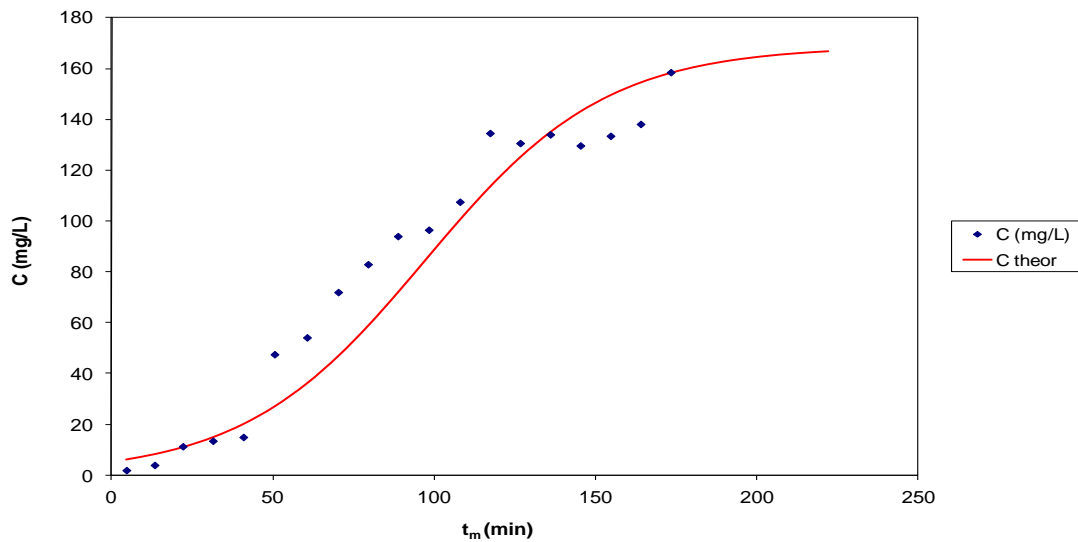


(b)

Fig. 14: Column experimental data and theoretical curves of MB adsorption on modified spruce; the effluent concentration is presented vs. (a) the effluent volume and (b) the adsorption time; $x=15\text{cm}$, $C_i=160\text{ mg L}^{-1}$, $Q=20\text{ mL min}^{-1}$, (the theoretical curves are according to the Bohart and Adams model); modified by brine treatment; concentrated x 4 times at $240\text{ }^\circ\text{C}$ for 50 min (repeatability).

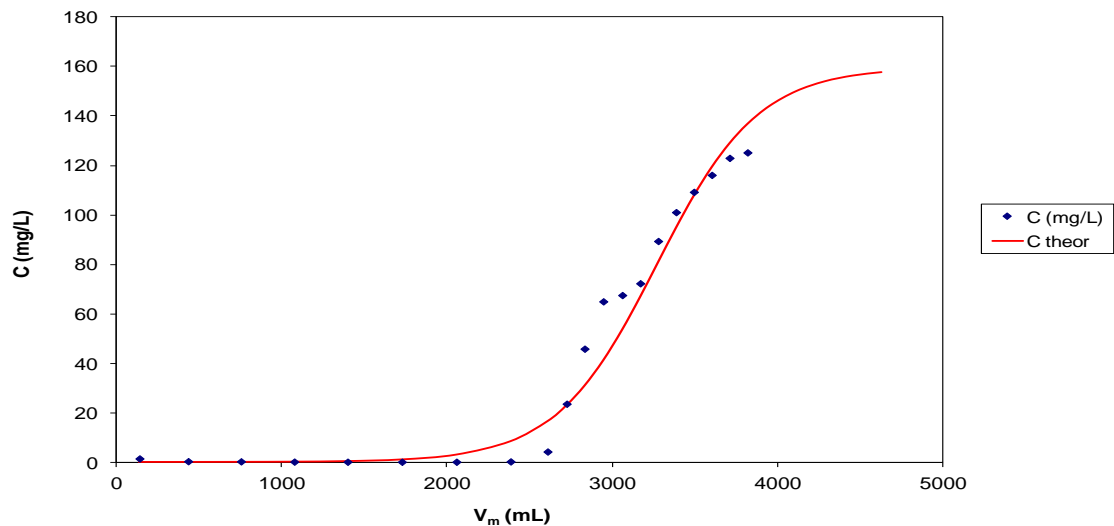


(a)

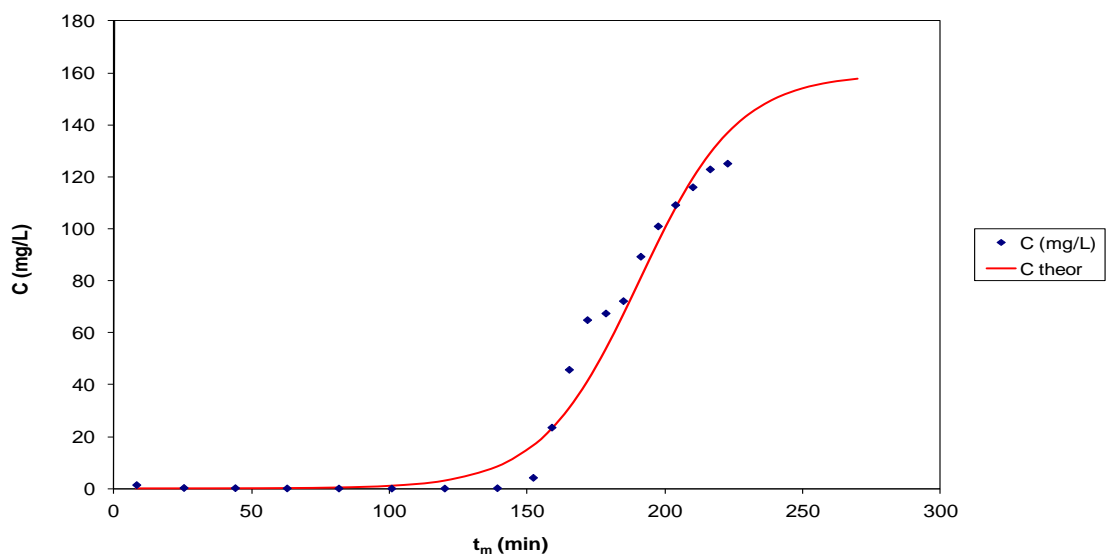


(b)

Fig. 15: Column experimental data and theoretical curves of MB adsorption on modified spruce; the effluent concentration is presented vs. (a) the effluent volume and (b) the adsorption time; $x=15\text{cm}$, $C_i=160\text{ mg L}^{-1}$, $Q=20\text{ mL min}^{-1}$, (the theoretical curves are according to the Bohart and Adams model); modified by brine treatment; concentrated x 8 times at $180\text{ }^\circ\text{C}$ for 0 min.

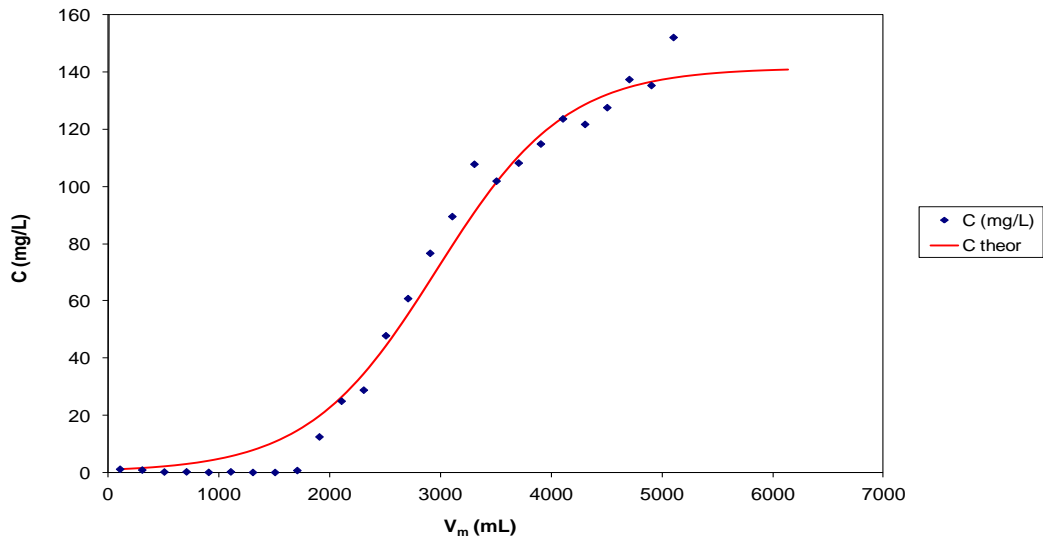


(a)

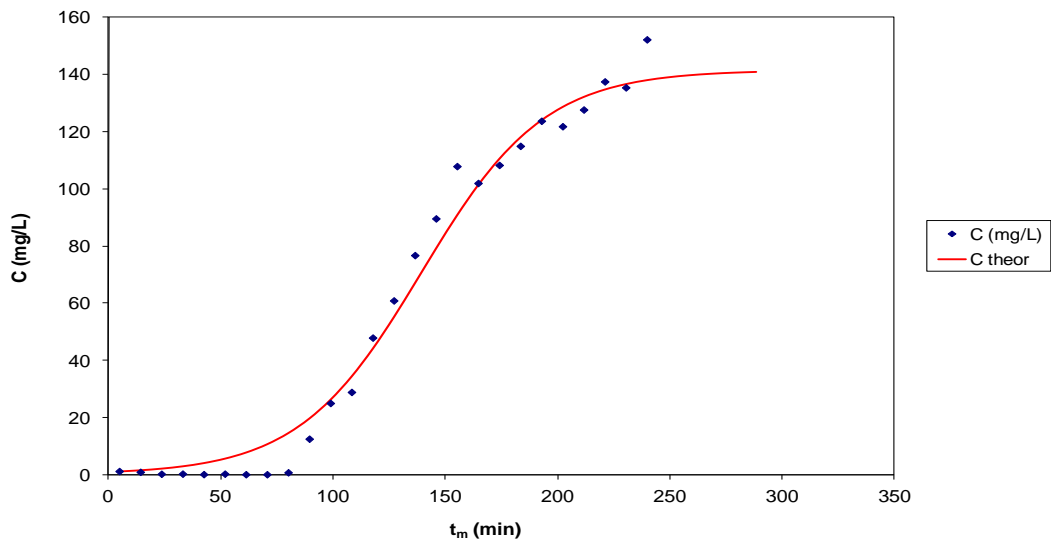


(b)

Fig. 16: Column experimental data and theoretical curves of MB adsorption on modified spruce; the effluent concentration is presented vs. (a) the effluent volume and (b) the adsorption time; $x=15\text{cm}$, $C_i=160\text{ mg L}^{-1}$, $Q=20\text{ mL min}^{-1}$, (the theoretical curves are according to the Bohart and Adams model); modified by brine treatment; concentrated x 8 times at $180\text{ }^\circ\text{C}$ for 50 min.



(a)



(b)

Fig. 17: Column experimental data and theoretical curves of MB adsorption on modified spruce; the effluent concentration is presented vs. (a) the effluent volume and (b) the adsorption time; $x=15\text{cm}$, $C_i=160\text{ mg L}^{-1}$, $Q=20\text{ mL min}^{-1}$, (the theoretical curves are according to the Bohart and Adams model); modified by brine treatment; concentrated x 8 times at $180\text{ }^\circ\text{C}$ for 50 min (repeatability).

4. References

- [1] M. Rafatullah, O. Sulaiman, R. Hashim, A. Ahmad, Adsorption of methylene blue on low-cost adsorbents: A review, *J. Hazard. Mater.* 177 (2010) pp. 70–80
- [2] A.M. El-Sayed, V. Mitchell, L-A. Manning, L. Cole, and D.M. Suckling, New sex pheromone blend for the lightbrown apple moth, *Epiphyas postvittana*, *J. Chem. Ecol.*, 37 (2011) pp. 640-646
- [3] S. Altenor, M.C. Ncibi, E. Emmanuel, S. Gaspard, Textural characteristics, physiochemical properties and adsorption efficiencies of Caribbean alga *Turbinaria turbinata* and its derived carbonaceous materials for water treatment application, *Biochem. Eng. J.* 1 67 (2012) pp. 35– 44
- [4] T. Liu, Y. Li, Q. Du, J. Sun, Y. Jiao, G. Yang, Z. Wang, Y. Xia, W. Zhang, K. Wang, H. Zhu, D. Wu, Adsorption of methylene blue from aqueous solution by grapheme, *Colloids and Surf. B: Biointerfaces.* 90 (2012) pp. 197– 203
- [5] Z.A. Al-Anber, M.A. Al-Anber, M. Matouq, O. Al-Ayed, N.M. Omari, Defatted Jojoba for the removal of methylene blue from aqueous solution: Thermodynamic and kinetic studies, *Desalination* 276 (2011) pp. 169–174
- [6] M. Malekbala, S. Hosseini, S.K. Yazdi, S. Masoudi Soltani, The study of the potential capability of sugar beet pulp on the removal efficiency of two cationic dyes, *Chem. Eng. Res. Des.* 90 (2012) pp.704–712
- [7] S.K. Theydan, M.J. Ahmed, Adsorption of methylene blue onto biomass-based activated carbon by FeCl₃ activation: Equilibrium, kinetics, and thermodynamic studies, *J. Anal. Appl. Pyrol.* 97 (2012) pp. 116–122

- [8] M.J. Ahmed, S.K. Dhedanb, Equilibrium isotherms and kinetics modeling of methylene blue adsorption on agricultural wastes-based activated carbons, *Fluid Phase Equilib.* 317 (2012) pp. 9–14
- [9] W.E. Oliveira, A.S. Franca, L.S. Oliveira, S.D. Rocha, Untreated coffee husks as biosorbents for the removal of heavy metals from aqueous solutions, *J. Hazard. Mater.* 152 (2008) pp. 1073–1081
- [10] A. Reffas, V. Bernardet, B. David, L. Reinert, M. Bencheikh Lehocine, M. Dubois, N. Batisse, L. Duclaux, Carbons prepared from coffee grounds by H_3PO_4 activation: Characterization and adsorption of methylene blue and Nylosan Red N-2RBL. *J. Hazard. Mater.* 175 (2010) pp. 779–788
- [11] M.H. Baek, C.O. Ijagbemi, O. Se-Jin, D.S. Kim, Removal of Malachite Green from aqueous solution using degreased coffee bean, *J. Hazard. Mater.* 176 (2010) pp. 820–828
- [12] G.Z. Kyzas, N.K. Lazaridis, A.Ch. Mitropoulos, Removal of dyes from aqueous solutions with untreated biomass as potential low-cost adsorbents: Equilibrium, reuse and thermodynamic approach, *Chem. Eng. J.* (2012) pp. 189–190, 148–159
- [13] H.M.F. Freundlich, Über die adsorption in lösungen, *Zeitschrift für Physikalische, Chemie.* 57 (1906) pp. 385-471
- [14] I. Langmuir, The constitution and fundamental properties of solids and liquids, *J. Am. Chem.Soc.* 38 (1916) pp. 2221-2295
- [15] R. Sips, Structure of a catalyst surface, *J. Chem. Phys.* 16 (1948) pp.490-495
- [16] S. Lagergren, Zur theorie der sogenannten adsorption gelöster stoffe, *Kungliga Svenska Vetenskapsakademiens, Handlingar* 24 (1898) pp.1-39

- [17] Y.S. Ho, J.C.Y. Ng, G. McKay, Kinetics of pollutants sorption by biosorbents: review, *Sep. Purif. Methods*. 29 (2000) pp. 189-232
- [18] W.J. Weber, J.C. Morris, Kinetics of adsorption on carbon from solution, *J. Sanit. Eng. Div. Am. Soc. Civ. Eng.* 89 (1963) pp.31–60
- [19] G. Bohart, E.N. Adams, Some aspects of the behavior of charcoal with respect to chlorine, *J. Am. Chem. Soc.* 42 (1920) pp. 523–544
- [20] R.M. Clark, Modeling TOC removal by GAC: The general logistic function, *J. Am. Wat. Works Assoc.* 79 (1987) pp. 33-37
- [21] M. Zhao, J.R. Duncan, R.P. Van Hille, Removal and recovery of zinc from solution and electroplating effluent using *Azolla filiculoides*, *Water Res.* 33 (1999) pp. 516–1522
- [22] E.Malkoc, Y.Nuhoglu, Cr (VI) adsorption bywaste acorn of *Quercus Ithaburensis* in fixed beds: prediction of breakthrough curves, Y. abali, *Chem. Eng. J.* 119 (2006) pp. 61–68
- [23] V. Vinodhini, Nilanjana Das,Packed bed column studies on Cr (VI) removal from tannery wastewater by neem sawdust. *Desalination* 264 (2010) pp. 9–14
- [24] F. Batzias, D. Sidiras, E. Schroeder, C. Weber, Simulation of dye adsorption on hydrolyzed wheat straw in batch and fixed-bed systems, *Chem. Eng. J.* 148 (2009) pp. 459–472
- [25] F. Batzias, D. Sidiras, E. Schroeder, C. Weber, Simulation of dye adsorption on hydrolyzed wheat straw in batch and fixed-bed systems, *Chem. Eng. J.* 148 (2009) pp. 459–472

- [26] W. Zhang, H. Yang, L. Dong, H. Yan, H. Li, Z. Jiang, X. Kan, A. Li, R. Cheng, Efficient removal of both cationic and anionic dyes from aqueous solutions using a novel amphoteric straw-based adsorbent, *Carbohydr. Polym.* 90 (2012) pp. 887–893
- [27] M.A. Ahmad, N.K. Rahman, Equilibrium, kinetics and thermodynamic of Remazol Brilliant Orange 3R dye adsorption on coffee husk-based activated carbon, *Chem. Eng. J.* 170 (2011) pp. 154–161
- [28] A.S. Franca, L.S. Oliveira, M.E. Ferreira, Kinetics and equilibrium studies of methylene blue adsorption by spent coffee grounds, *Desalination* 249 (2009) pp. 267–272
- [29] L. Wang, Z. Huang, M. Zhang, B. Chai, Adsorption of methylene blue from aqueous solution on modified ACFs by chemical vapor deposition, *Chem. Eng. J.* (2012) pp. 189–190, 168–174
- [30] M.U. Dural, L. Cavas, S.K. Papageorgiou, F.K. Katsaros, Methylene blue adsorption on activated carbon prepared from *Posidonia oceanica* (L.) dead leaves: Kinetics and equilibrium studies, *Chem. Eng. J.* 168 (2011) pp. 77–85